Chapter 15
Optimization of Windspeed Prediction Using an Artificial Neural Network Compared With a Genetic Programming Model

Ravinesh C. Deo
University of Southern Queensland, Australia

Sujan Ghimire
University of Southern Queensland, Australia

Nathan J. Downs
University of Southern Queensland, Australia

Nawin Raj
University of Southern Queensland, Australia

ABSTRACT

The precise prediction of windspeed is essential in order to improve and optimize wind power prediction. However, due to the sporadic and inherent complexity of weather parameters, the prediction of windspeed data using different patterns is difficult. Machine learning (ML) is a powerful tool to deal with uncertainty and has been widely discussed and applied in renewable energy forecasting. In this chapter, the authors present and compare an artificial neural network (ANN) and genetic programming (GP) model as a tool to predict windspeed of 15 locations in Queensland, Australia. After performing feature selection using neighborhood component analysis (NCA) from 11 different metrological parameters, seven of the most important predictor variables were chosen for 85 Queensland locations, 60 of which were used for training the model, 10 locations for model validation, and 15 locations for the model testing. For all 15 target sites, the testing performance of ANN was significantly superior to the GP model.

DOI: 10.4018/978-1-5225-4766-2.ch015

1. INTRODUCTION

The fluctuation of the wind heavily affects wind power generation. Therefore, accurate wind forecasting models are very important for effective wind power systems management. Among all the renewable energy sources, windspeed needs more forecasting approaches than currently implemented due to its higher intermittency rate (Masrur, Nimol, Faisal, & Mostafa, 2016). In the literature, three different methods have been introduced for windspeed (Ws) forecasting: physical, statistical and hybrid (Foley, Leahy, Marvuglia, & McKeogh, 2012). Physical methods are based on principles of physics such as the numerical weather prediction (NWP) models. Statistical models can be as simple as persistence to more complicated models such as Artificial Neural Networks (ANN) (Blonbou, 2011) or Markov chains. Hybrid methods combine physical and statistical models like the Autoregressive Integrated Moving Average Model (ARIMA) and ANN, which can generate non-linear functions to create an accurate model capable of predicting time series of windspeed and wind power output.

Many studies with several different models were done for diverse regions around the world. The ARIMA model was proposed by Benth and Benth (Benth & Benth, 2010) for forecasting the windspeed for three different wind farms in New York state. Zhu and Genton (Zhu & Genton, 2012) reviewed statistical short-term windspeed forecasting models, including autoregressive models and traditional time series approaches used in wind power developments to determine which model provided the most accurate forecasts. Due to the nonlinearity pattern of wind data, the forecasts using ARIMA may have inaccuracies because the ARIMA model is a linear series model (Cadenas & Rivera, 2010). Therefore, ANN has been applied to handle the nonlinear nature of windspeed data in previous research. A comparison of ANN and ARIMA was presented by Cadenas and Rivera (Cadenas & Rivera, 2007) using seven years of windspeed data. Six years of this dataset were used for the training, and one year for the validation, using performance metrics like Mean Square Error (MSE) and Mean Absolute Error (MAE). These were found to be lower for ANN when compared with ARIMA. Similarly, daily, weekly and monthly windspeed was forecasted using data from four different measuring stations in the Aegean and Marmara regions of Turkey by Bilgili and Sahin (Bilgili & Sahin, 2013). The results show that the ANN forecast was superior. In addition to this, recently Zameer et al. (Zameer, Arshad, Khan, & Raja, 2017), proposed the Genetic Programming (GP) model for the short term prediction of wind for five different wind farms in Europe, the average root MSE was 0.1176 ms^{-1}.

A challenge for the machine learning (ML) models is the requirement of the input data that must be related to the target variable. These input variables are not often available easily due to the remoteness of potential sites and the cost and maintenance associated with the experimental apparatus. Fortunately, Meteorological reanalysis have arisen as an important data source for renewable energy modeling studies over the past few years for several reasons: reanalysis data are usually available globally; they provide several decades of coverage; and they are usually freely available. Commonly used global reanalysis of the most recent generation include MERRA (Modern-Era Retrospective Analysis for Research and Applications), re-analysis proposed by NASA's (National Aeronautics and Space Administration) Global Modeling and Assimilation Office (Rienecker, Suarez, Gelaro, Todling, Bacmeister, Liu, & . . . Kim, 2011), the ERA-Interim re-analysis of the ECMWF (European Centre for Medium-range Weather Forecasts) (Dee et al., 2011) and the Japanese 55-year reanalysis (JRA-55) (Kobayashi, Ota, Harada, Ebita, Moriya, Onoda, & . . . Takahashi, 2015). There is a wide range of recent work done by using reanalysis data for wind power simulation (e.g. Refs. (Staffell & Green, 2014).

In our study, we have developed two ML models, ANN and GP to predict *Ws* for 15 locations in Queensland, Australia. ANN and GP is an appropriate method for wind power prediction and has been widely used (Alexiadis, Dokopoulos, Sahsamanoglou, & Manousaridis, 1998; Fan, Wang, Liu, & DAI, 2008; Kariniotakis, Stavrakakis, & Nogaret, 1996; Mohandes, Rehman, & Halawani, 1998; Seo & Hyeon, 2015) in renewable energy prediction. In order to form the ML model, monthly average values of metrological parameters for 85 locations in Queensland were extracted from the surface meteorology and solar energy release 6.0 (SSE 6.0) (Stackhouse & Whitlock, 2009). This data was obtained from the NASA Science Mission Directorate's satellite and re-analysis research programs which extends the temporal coverage of the solar and meteorological data from 10 years to more than 22 years. A total of 60 cities of the Queensland region were used for training, 10 cities for the validation and 15 cities for testing. Before feeding the ANN and GP model, feature selection was performed to optimize the selection of predictor variables.

2. METHODOLOGY

Table 1 shows the list of predictor variables extracted from SSE 6.0. Combinations of these variables were used for the long-term prediction of *Ws*. The monthly average values for each these variables were taken as input for the feature selection.

2.1 Artificial Neural Network

In this study, we applied an artificial neural network based multilayer perceptron (MLP) algorithm to examine the problem of windspeed forecast. Briefly, the MLP model is one of the most common neural network architectures, utilizing a feedforward backpropagation (FFBP) network. The basic advantages of ANN over the conventional correlations is neural networks have large degrees of freedom for fitting parameters and thus, capture the systems' non-linearity better than regression methods. Furthermore, ANN can be further trained and refined when additional data become available in order to improve their

Table 1. Description of the extensive pool of predictor variables and notations

S.N.	Predictor Variable	Abbreviation	Unit
1	Latitude	Lat	Deg
2	Longitude	Long	Deg
3	Elevation	Elev	m
4	Air temperature	T_{air}	Deg C
5	Relative humidity	RH	%
6	Daily solar radiation - horizontal	I_{rad}	$kWhm^{-2}d^{-1}$
7	Atmospheric pressure	Patm	kPa
8	Earth temperature	E_{Temp}	Deg C
9	Heating degree-days	HDD	Deg C
10	Cooling degree-days	CDD	Deg C

prediction accuracy while it is impossible to make any further change in a linear or non-linear regression model as soon as a model development is over (Farshad, Garber, & Lorde, 2000; Gharbi & Elsharkawy, 1996; Gharbi & Elsharkawy, 1997; Makinde, Ako, Orodu, & Asuquo, 2012). The FFBP model has been applied in many previous studies of renewable energy (e.g., Ravinesh C Deo & Sahin, 2017; Ghorbani, Khatibi, Hosseini, & Bilgili, 2013). The FFBP model offers a competent learning environment that minimizes error between the target and the obtained values (Ul-Saufie, Yahaya, Ramli, Rosaida, & Hamid, 2013). As shown in Figure 1 the network of FFBP usually consists of an input layer (X_1, X_2, X_3,..X_n), several hidden layers, and an output layer (Y). Each layer consists of several operating neurons, each of which is connected to every neuron in nearby layers through adaptable synaptic weights that determine the strength of the relationship between two connected neurons. In each layer, every neuron sums all the inputs that have been received from previous layers and forms the neuron output through a predefined activation or transfer function. Learning is defined as the ability of a network to change weights by application of a backpropagation algorithm through two phases. In the forward phase, the training data set is propagated through the hidden layer and comes out of the neural network through the output layer. The output values are then compared with actual target output values. The error between the output layer and the actual values are calculated and propagated back toward the hidden layer (Elbayoumi, Ramli, & Fitri Md Yusof, 2015). In the backward phase, derivatives of network error (with respect to the networks) are fed back to the network and used to adjust the weights to reduce errors with each iteration, thus improving the FFBP models and prompting the neural model to produce the desired outputs.

The network construction in this study consists of three-layer perceptron model. The first input layer contains the input variables that were selected by neighborhood component analysis (Yang, Wang, & Zuo, 2012) feature selection "*fsrnca*" method to reduce complexity by retaining fewer variables. The second architecture layer is the hidden layer. The common problems in hidden layer architecture are to identify the number of hidden layers, to identify neurons values and to choose the suitable activation function. The optimum number of neurons is important because too few neurons will contribute to

Figure 1. ANN network construction adopted for daily windspeed forecast, X_1, X_2, X_3,.....X_n are input variables and y is the output variable.

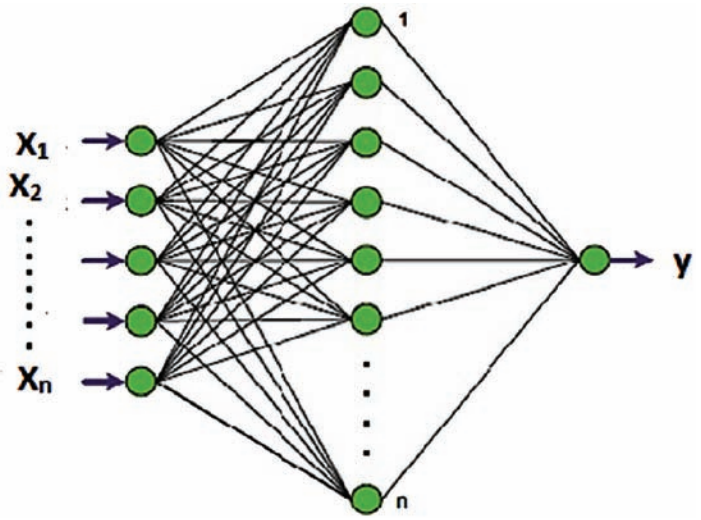

under-fitting, whereas too many neurons lead to overfitting. A fixed scientific solution for the design of an optimal ANN model does not exist. Using Equation 1, the initial number of neurons will be found and the number was increased until a stable and optimal value was achieved.

$$n_h = 2 \times n_i + 1$$

where, n_i is the number of input neurons, and n_h is the number of hidden neurons.

The second problem in building the architecture of the hidden layer is deciding suitable transfer function. According to Kriesel (Kriesel, 2007), the transfer function in the hidden layers must use a nonlinear transfer function (otherwise the result end up with only linear separable solutions). Therefore, the optimal activation functions are obtained using sigmoid transfer function (Ul-Saufie, Yahaya, Ramli, Rosaida, & Hamid, 2013). The most common sigmoid functions are linear (purelin), log-sigmoid (logsig) and hyperbolic tangent sigmoid (tansig). The logistic function will generate values close to 0. If the argument of the function is negative, the output of hidden neuron will be close to zero, and as a result lowering the learning rate for all subsequent weights-will almost stop learning. Tansig can produce both positive and negative values which will generate a value close to -1.0, and thus will maintain learning (Kriesel, 2007). In this study, tansig, logsig and purelin functions were used to build the architecture of the hidden layer. The third architecture layer is the output layer which consists of the target of the forecasting model which is the windspeed.

The ANN algorithm can be formulated as (REF):

$$Y(X) = F\left(\sum_{i=1}^{L} w_i\,(t).X_i(t) + b\right)$$

$$\text{Tangent Sigmoid} \Rightarrow F(X) = \frac{2}{1+\exp(-2X)} - 1$$

$$\text{Log Sigmoid} \Rightarrow F(X) = \frac{1}{1+\exp(-X)}$$

$$\text{Linear=linear(x)=x}$$

where $X_i(t)$ is representing predictor/forecasting (input) variable(s) in discrete time space t while $Y(x)$ is referred to a forecasted *windspeed (Y)* in (test) data set. Moreover, L is the number of hidden neurons that determined iteratively after finding the initial hidden neuron from Equation 1, $w_j\,(t)$ is the weight which connects the i^{th} neuron in the input layer. In Equation 2, b is used a neuronal bias and $F(.)$ is the function of hidden transformation in the ANN network architecture.

Since an ANN model is a black-box and does not identify the training algorithm in an explicit manner without an iterative model identification process, this study has tested several algorithms whose performances were assessed to select the best model. In our study, six types of training algorithms are used. The quick processing algorithms used as a technique for numerical optimization such as Conjugate Gradient back propagation with Polak-Ribiere (traincgp), Scaled Conjugate Gradient (trainscg), One Step Secant Backpropagation Algorithm (trainoss), Broyden–Fletcher–Goldfarb–Shann (trainbfg),

Conjugate Gradient Backpropagation with Fletcher-Reeves Updates (traincgf) and Levenberg–Marquardt Backpropagation (trainlm) (MathWorks, 1996).

The *traincgp* algorithm, is the ratio of the inner product of the previous change in the gradient with the present gradient to the norm squared of the last gradient (Hagan, Demuth, & Beale, 1996; Møller, 1993), whereas the *traincgf* algorithm is the ratio of the norm squared of the current gradient to the norm squared of the previous gradient. In the first iteration, the conjugate gradient algorithm will find the steep descent direction. Approximate solution, 'X_k' for conjugate gradient iteration is described as formulas below (Ojha, Dutta, Chaudhuri, & Saha, 2013).

$$X_k = X_{k+1} + \alpha_k \cdot d_k$$

where, learning rate αk is determined using line search algorithm such that

$$SSE(X_k + \alpha_k g_k) \leq SSE(g_k)$$

where, 'd_k' is the search direction basically $d_k = -g_k$, where g_k is gradient computed based on 'X_k'. Note that,

$$d_k = \begin{cases} -g_k & k = 0 \\ -g_k + \beta_k d_{k-1} & Otherwise \end{cases}$$

where, β_k is a factor which scales the influence previous gradient analogous to momentum factor in backpropagation.

The different methods employed in the computation of β_k leads to different versions of conjugate gradient methods.

For *traincgf* and *traincgp,* the β_k is calculated as per Equation [7] and Equation [8] respectively. Where, $y_{k-1} = g_k - g_{k-1}$:

$$\beta_k = \frac{\left\|g_k\right\|^2}{\left\|g_{k-1}\right\|^2}$$

$$\beta_k = \frac{g_k^T y_{k-1}}{\left\|g_{k-1}\right\|^2}$$

The conjugate gradient algorithms are usually much faster than other algorithms but the result depends on the problem (Fletcher & Reeves, 1964). As compared to traincgf, the storage necessities for traincgp are quite larger (Sharma & Venugopalan, 2014).

The *trainscg* (Hagan, Demuth, & Beale, 1996; Møller, 1993) is formulated to avoid the time consumption in line search at each iteration of other conjugate gradient algorithms. It is used as general-purpose training algorithms.

The *trainbfg* algorithm approximates Newton's method, a class of hill-climbing optimization techniques that seeks a stationary point of a function. For such problems, a necessary condition for optimality is that the gradient be zero (MathWorks, 1996).

The basic step of Newton's method is:

$$X_{k+1} = X_k - A_k^{-1}.g_k$$

where, A_k^{-1} is the Hessian matrix (second derivatives) of the performance index at the current values of the weights and biases. Newton's method often converges faster than conjugate gradient methods. Unfortunately, it is complex and expensive to compute the Hessian matrix for feedforward neural networks. There is a class of algorithms that is based on Newton's method, but it does not require calculation of second derivatives. These are called quasi-Newton (or secant) methods. They update an approximate Hessian matrix at each iteration of the algorithm. The update is computed as a function of the gradient trainbfg updating method and the trainlm algorithms avoid this difficulty because they update an approximate Hessian matrix at each iteration of the algorithm. Levenberg–Marquardt algorithm was designed to approach second-order training speed without having to compute the Hessian matrix. If the performance function has the form of a sum of squares, then the Hessian matrix can be approximated as (Sharma & Venugopalan, 2014). If the performance function has the form of a sum of squares, then the Hessian matrix can be approximated as:

$$H = J^T J$$

and the gradient can be computed as:

$$g = J^T e$$

Where '*J*' is the Jacobian matrix that contains first derivatives of the network errors with respect to the weights and biases, and '*e*' is a vector of network errors. The Jacobian matrix can be computed through a standard back propagation technique that is much less complex than computing the Hessian matrix. The Levenberg–Marquardt algorithm uses this approximation to the Hessian matrix in the following Newton-like update:

$$X_{k+1} = X_k - \left[J^T J + \mu I\right]^{-1} J^T e$$

When the scalar 'μ' is zero, this is just Newton's method, using the approximate Hessian matrix. When 'μ' is large, this becomes gradient descent with a small step size. Newton's method is faster and more accurate near an error minimum, so the aim is to shift towards Newton's method as quickly as possible. Thus, 'μ' is decreased after each successful step that is reduction in performance function and is increased only when a tentative step would increase the performance function.

The *trainbfg* have superior performance even for non-smooth optimizations and an efficient training function for smaller networks whereas the *trainlm* algorithm locates the minimum of a multivariate function that can be expressed as the sum of squares of non-linear real-valued functions. It is an iterative technique that works in such a way that performance function will always be reduced in each iteration of the algorithm. This feature makes *trainlm* back propagation optimization learning algorithm is the most rapid learning algorithm tool for moderate size network (Kamble, Pangavhane, & Singh, 2015). Both *trainbfg* and *trainlm* function has drawback of memory and computation overhead caused due to the calculation of the gradient and approximated Hessian matrix (Pham & Sagiroglu, 2001).

The *trainoss* algorithm is an improved method of trainbfg algorithm as it decreases the calculation and storage at each iteration. The *trainoss* method does not store the complete Hessian matrix; it assumes that the previous Hessian matrix was the identity matrix. This function has additional advantage that the new search direction can be calculated without computing a matrix inverse. So, *trainoss* is considered a compromise between full quasi-Newton algorithms and conjugate gradient algorithms (Kamble, Pangavhane, & Singh, 2015).

2.2 Multi- Gene Genetic Programming

Genetic Programming (GP) uses principle of genetic algorithms (GA) to evolve computer programs/ models of varying sizes based on Darwinian Theory of "Survival of the fittest" (Koza, 1994). Although both GP and GA share the same working principle but there exists difference between them. The GP represents the problem solution as a tree in a symbolic form (Poli, Langdon, & McPhee, 2008; Raja, 2008) whereas GA evolves solutions represented by strings (binary or real number) of fixed length (Garg, Vijayaraghavan, Mahapatra, Tai, & Wong, 2014). Figure 2 below illustrates the main parts of GP approach. As shown, in the first step, the GP creates an initial population (individuals) based on a random search of space. Each individual, also called program, has a symbolic tree structure and is made up of predefined functions set and terminals. At next step, the fitness function is used to evaluate each individual of population. After that, with respect to the Darwinian principle (reproduction of the fittest individual), the new generation will be created by using three genetic operators, namely crossover, mutation and reproduction.

The most common method of recombination is *crossover*. In this method two parents swap randomly selected sub-trees to produce two children. *Mutation* involves replacing the sub-tree with a new randomly generated tree at a mutation point. *Reproduction* selects the fitter individuals and repeats them into next generation with no change. After applying genetic operators, the new population is evaluated for fitness. This process will continue until criterion is satisfied that is finding the optimized individual, or reaching predefined number of generations. Another important aspect in GP is choosing the individuals for recombination. Different methods for individual selection have been proposed. The two common methods are fitness selection and tournament selection. In first method, each individual has a chance to be selected in accordance with its fitness, whereas in the second method, a small number of individuals compete in a fitness tournament to be selected for recombination (Rahdari, Eftekhari, & Mousavi, 2016).

When the algorithm creates a number of genes rather than one, it is called *multi-gene symbolic regression* which is a more accurate technique applied for producing a population of mathematical relation (Abhishek, Panda, Datta, & Mahapatra, 2014). A multi-gene consists of one or more genes which are individually usual GP trees. Thus, multi-gene genetic programming (MGGP) approaches often give simpler functions than other models consisting of one monolithic GP tree (Abooali & Khamehchi, 2014).

A free open source GP toolbox called "GPTIPS "software is used for the implementation of GP. This software is a new "Genetic Programming and Symbolic Regression" code written based on MGGP (Hinchliffe, Hiden, McKay, Willis, Tham, & Barton, 1996; Searson, Leahy, & Willis, 2010) for the use with MATLAB (MathWorks, 1996). In GPTIPS, there are some adjustable parameters like the maximum number of genes in the regressing process, primary mathematical operators, number of population and so on which should be determined before the run by user. The structure of multigene symbolic regression models is illustrated in Figure 3.

The prediction of the y training data is given by:

$$\hat{y} = b_0 + b_1 t_1 + \ldots\ldots\ldots\ldots\ldots + b_G t_G$$

where t_i is the (N × 1) vector of outputs from the i^{th} tree/gene comprising a multigene individual. Next, define G as a (N × (G + 1)) gene response matrix as follows in Equation [14].

$$G = [1 t_1 \ldots\ldots\ldots\ldots t_g]$$

where, the **1** refers to a (N × 1) column of ones used as a bias/offset input.

Now, Equation [13] can be written as:

$$\hat{y} = Gb$$

The least squares estimate of the coefficients b_0, b_1, b_2,..., b_G formulated as a *((G + 1) × 1)* vector can be computed from the training data as Equation [16]:

$$b = (G^T G)^{-1} G^T y$$

In practice, the columns of the gene response matrix ***G*** may be collinear (e.g. due to duplicate genes in an individual, and so the Moore-Penrose pseudo-inverse (by means of the singular value decomposition; SVD) is used in Equation [16] instead of the standard matrix inverse. Because this is computed for every individual in a GPTIPS population at each generation (except for cached individuals), the computation of the gene weighting coefficients represents a considerable proportion of the computational expense of a run. In GPTIPS, the RMSE is then calculated from SSE and is used as the fitness/objective function that is minimized by the MGGP algorithm.

Figure 2. Multigene symbolic regression. The prediction of the response data y is the vector output of G trees modified by bias term b0 and scaling parameters b_1, ..., b_G.

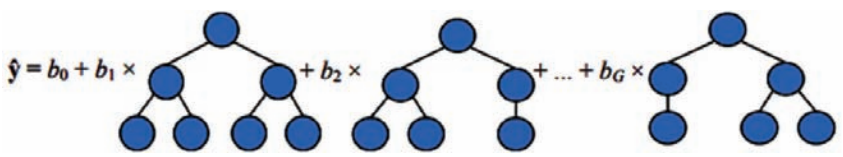

GPTIPS was used in this study in order to develop a non-linear correlation for Ws. Input data (training, validation and test sets) after the feature selection process "fsrnca" were feed to the GPTIPS program. Then, tuning parameters of the code were adjusted and modified. After running the program, the correlation was obtained with good statistical evaluation criteria and accuracy.

3. MODEL DEVELOPMENT

3.1 Data Normalization

For the construction of the ANN and GP model, the data was partitioned into three sets of training, validation, and testing, comprising 60 Queensland cities for training, 10 Queensland cities for validation and 15 Queensland cities for model testing. Figure 4 shows the map of Queensland with training, testing and validation sites, Table 2 illustrates the data segregation for the modelling purpose. Furthermore, all predictors as well as objective variables were normalized using a normalization method. Normalization

Figure 3. Flowchart describing the steps involved in a genetic programming approach.

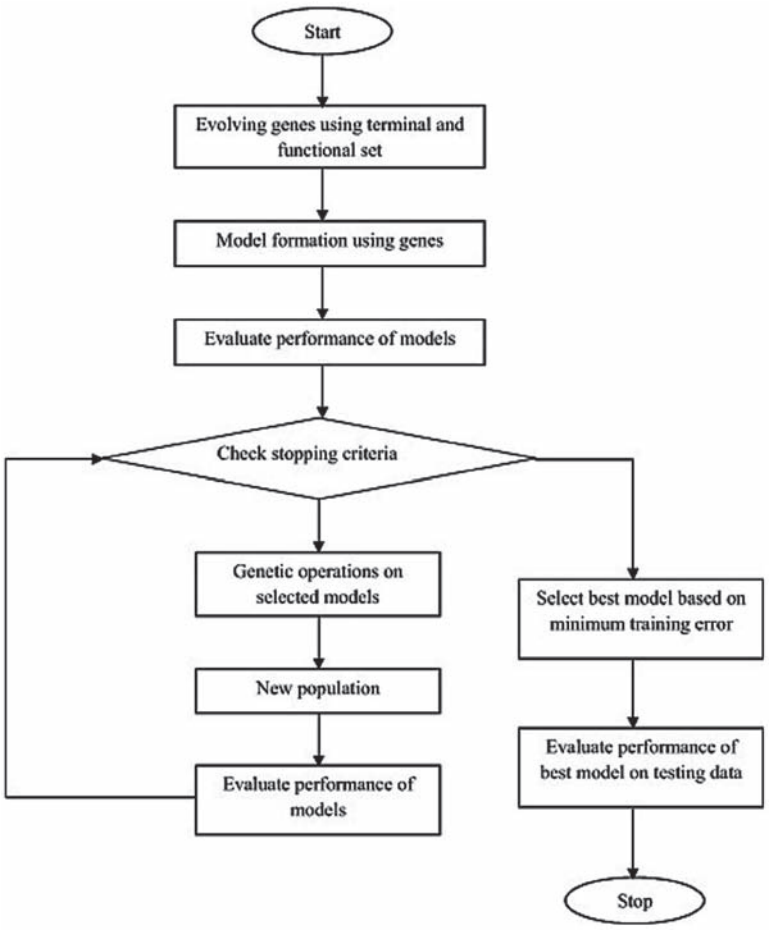

can be performed between 0 and 1 or -1 and 1. The normalization gives equal weight to all variables (Afram, Janabi-Sharifi, Fung, & Raahemifar, 2017); it was done to reduce the time of learning because of large fluctuations in data and to ensure that the predictor variables do not affect the process of model construction. The data were normalized between 0 and 1 according to the following Equation .

$$X_{norm} = \frac{X - X_{\min}}{X_{\max} - X_{\min}}$$

where, $X_{norm}, X_{\max}$ and $X_{\min}$ represent the normalized, minimum, and maximum values of the variable X, respectively.

3.2 Feature Selection

To achieve a high forecasting accuracy an optimal selection of input variables is vital. This is because there are often some features in the training datasets that might not be relevant to the leaning task. Some might even be noisy and have a negative impact on the performance of the forecasting model. In general, the impact of the input variables can be found in different ways by considering their relevance, computational effort, training difficulty, dimensionality and comprehensibility (May, Dandy, & Maier, 2011). The optimal input variable set will contain the fewest predictive variables required to describe the

Figure 4. The present study area (showing cities) located in the Queensland region where artificial neural network and Genetic Programming model was used for forecasting Windspeed, Table 2 provides the details of the locations.

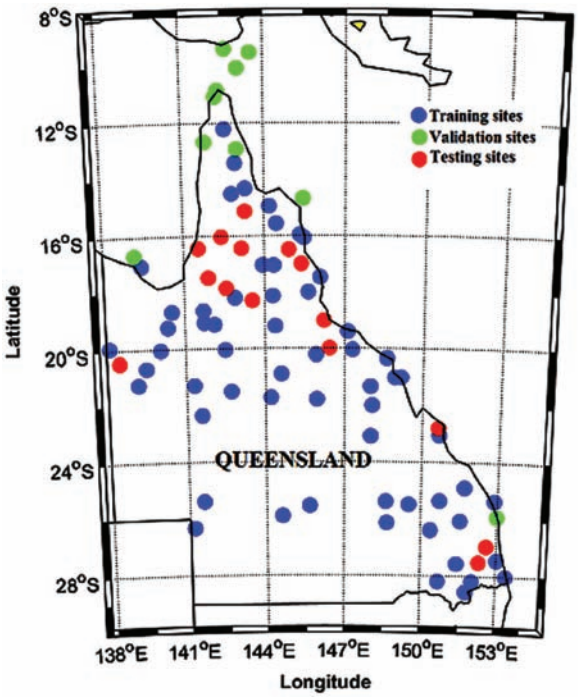

behavior of the objective variable, *Ws* with a minimum degree of redundancy and with no uninformative (noise) variables. Kim (Kim, 2015) explains that the identification of an optimal set of input variables will lead to a more accurate, efficient, cost-effective and more easily interpretable ML model. Hence, it is vital to take advantage of feature selection algorithms that can identify the features that are relevant and necessary for the learning problem. In our modelling, we started with 10 different inputs (Table 1) downloaded as predictor variables and have done feature selection using neighborhood component analysis for regression (NCA). NCA is a non-parametric and embedded method for selecting features with the goal of maximizing prediction accuracy of regression algorithms (Yang, Wang, & Zuo, 2012). The MATLAB function called "*fsrnca*" performs NCA feature selection with regularization to learn feature weights for minimization of an objective function that measures the average 'leave-one-out' regression loss over the training data.

The *fsrnca* function performs NCA feature selection modified for regression. Given *n* observations

$$S = \{(x_i, y_i), i = 1,2,.....n\},$$

where $x_i \in \mathbb{R}^p$ are the feature vectors, and $y_i = \mathbb{R}$ is a continuous function. The aim is to predict the response *y* given the training set *S*.

Consider a randomized regression model that:

- Randomly picks a point $(\mathrm{Re}\, f(x))$ from *S* as the 'reference point' for *x*.
- The function sets the response value at *x* equal to the response value of the reference point $(\mathrm{Re}\, f(x))$

Again, the probability $P(Ref(x) = x_j \mid S)$ that point x_j is picked from *S* as the reference point for *x* is higher if x_j is closer to *x* as measured by the distance function d_w, where:

$$d_w(x_i, x_j) = \sum_{r=1}^{p} w_r^2 \left| x_{ir} - x_{jr} \right|$$

And w_r are the feature weights, assuming that,

$$P(Ref(x) = x_j \left| S) \propto k(d_w(x, x_j)),\right.$$

where, *k* is some kernel or a similarity function that assumes large values when $d_w(x,x_j)$ is small. Suppose it is:

$$k(z) = \exp\left(-\frac{z}{\sigma}\right),$$

where the kernel width σ is an input parameter that influences the probability of each point being selected as the reference point. As suggested by Yang et al. (Yang, Wang, & Zuo, 2012), The reference

point for x is chosen from S, so the sum of $P(Ref(x) = x_j \mid S)$ for all j must be equal to 1. Therefore, it is possible to write:

$$P(Ref(x) = x_j \mid S) = \frac{k(d_w(x, x_j))n_j}{\sum_{j=1}^{N} k(d_w(x, x_j))}.$$

Now consider the 'leave-one-out' application of this randomized regression model that is predicting the response for x_i using the data in S^{-i}, and the training set S excluding the point (x_i, y_i). The probability that point x_j is picked as the reference point for x_i is:

$$p_{ij} = P(Ref(x_i) = x_j \mid S^{-1}) = \frac{k(d_w(x_i, x_j))}{\sum_{j=1, j\neq 1}^{N} k(d_w(x_i, x_j))}.$$

Let $\hat{y}_i$ be the response value the randomized regression model predicts and y_i be the actual response for x_i. Also let $l : \mathbb{R}^2 \rightarrow \mathbb{R}$ be a loss function that measures the disagreement between $\hat{y}_i$ and y_i. Then, the average value of $l(y_i, \hat{y}_i)$ is:

$$l_i = E(l(y_i, \hat{y}_i) \mid S^{-1}) = \sum_{j=1, j\neq 1}^{N} \text{probability that} \, x_j \, \text{is the reference point for} \, x_i \times l(y_i, y_j)$$
$$= \sum_{j=1, j\neq 1}^{N} p_{ij} l(y_i, y_j)$$

After adding the regularization term, the objective function for minimization is:

$$f(w) = \frac{1}{n} \sum_{i=1}^{n} l_i + \lambda \sum_{r=1}^{p} w_r^2.$$

The default loss function $l(y_i, y_j)$ for NCA for regression is the mean absolute deviation. The regularization term derives the weights of irrelevant predictors to zero. In the objective functions for NCA for regression, there is only one regularization parameter, λ for all weights. This fact requires the magnitudes of the weights to be comparable to each other. When the feature vectors x_i in S are in different scales, this might result in weights that are in different scales and not meaningful. To avoid this situation, normalization of data is necessary before applying NCA. Furthermore, it is usually necessary to select a value of the regularization parameter by calculating the accuracy of the randomized NCA regression model on an independent test set. If we use cross-validation instead of a single test set, the λ value should be selected in such a way that it minimizes the average loss across the cross-validation folds.

After doing the feature selection using "*fsrnca" a total of* 7 input predictors were selected based on highest weights for all Queensland locations. The selected predictor variables after performing NCA feature selection are presented in Table 3.

3.3 Performance Evaluation

To evaluate the performance of ANN as well as the GP model, several statistical metrics were employed. The mathematical representations are enumerated as follows. Where, ws_{OBS} and ws_{FOR} are the observed and forecasted i[th] value of *windspeed*, $\overline{ws}_{OBS}$ and $\overline{ws}_{FOR}$ are the observed and forecasted mean *windspeed* and *N* is the number of datum points in the test set.

1. **Correlation coefficient (r) expressed as:**

$$r = \left(\frac{\sum_{i=1}^{N} \left(ws_{OBS,i} - \overline{ws}_{OBS,i} \right) \left(ws_{FOR,i} - \overline{ws}_{FOR,i} \right)}{\sqrt{\sum_{i=1}^{N} \left(ws_{OBS,i} - \overline{ws}_{OBS,i} \right)^2} \sqrt{\sum_{i=1}^{N} \left(ws_{FOR,i} - \overline{ws}_{FOR,i} \right)^2}} \right)^2$$

The degree of collinearity between simulated and measured data ranges from −1 to 1 and is described by the correlation coefficient (*r*). If $r = 0$, no linear relationship exists. If $r = 1$ or -1, a perfect positive or negative linear relationship exists (Coimbra, Kleissl, & Marquez). The equation for *r*, however, is based on the consideration of a linear relationship between observed and simulated data.

2. **Root mean square error (RMSE) is expressed as:**

$$RMSE = \sqrt{\frac{1}{N} \sum_{i=1}^{N} \left(ws_{FOR,i} - ws_{OBS,i} \right)^2}$$

The RMSE is a frequently used measure to compare forecasting errors of different models. In this case the RMSE of the target variable, *Ws* is expressed in ms^{-1}. The lower RMSE value the better the predictive capability of a model in terms of its absolute deviation. However, presence of few large errors can result in a greater value of RMSE (Despotovic, Nedic, Despotovic, & Cvetanovic, 2016).

3. **Mean absolute error (MAE) is expressed as:**

$$MAE = \frac{1}{N} \sum_{i=1}^{N} \left| \left(ws_{FOR,i} - ws_{OBS,i} \right) \right|$$

Table 2. Data sets used for study

Dataset of 60 locations of Queensland used for training							
S.N	City	Lat(Deg.)	Long(Deg.)	S.N	City	Lat(Deg.)	Long(Deg.)
1	Lyndhurst	-19.206578	144.36992	31	Camooweal	-19.92177	138.11912
2	Mount Surprise	-18.1477	144.3161	32	Cape Tribulation	-16.0793	145.4683
3	Bapaume	-28.566	151.829	33	Albion	-21.50903	142.69317
4	Prairie	-20.870948	144.60234	34	Gilbert River	-18.1942	142.88228
5	Rookwood	-17.041443	144.34203	35	Middleton	-22.35368	141.55175
6	Upper Dawson	-25.411517	148.6366	36	Mount Jukes	-21.00082	148.93189
7	Kooroomool	-18.005233	145.63586	37	Millaroo	-20.05802	147.28172
8	Balfes Creek	-20.21594	145.9095	38	East Creek	-19.07725	141.70175
9	Bongeen	-27.568	151.447	39	Four Ways	-19.23309	140.3413
10	Womina	-28.190571	152.04626	40	Takilberan	-24.88231	151.68471
11	Wyaga	-28.20612	150.70529	41	Laura	-15.55963	144.4449
12	Eumamurrin	-26.156521	148.6575	42	Bungundarra	-23.06272	150.65611
13	Broadmere	-25.494713	149.52529	43	Bundall	-28.00417	153.40684
14	Scrubby Creek	-25.541515	145.66424	44	Strathdickie	-20.32937	148.61146
15	Pelham	-26.408864	150.37302	45	Booral	-25.35272	152.89079
16	Speedwell	-26.066559	151.54742	46	Farrars Creek	-25.39361	141.55373
17	Tangorin	-21.726606	144.2029	47	Claraville	-18.66251	141.70554
18	Buchanan	-21.793411	145.94017	48	Wanjuru	-17.46744	146.06597
19	Eidsvold West	-25.362586	150.71895	49	Royal Brisbane Hospital	-27.448	153.027
20	Arbouin	-17.027167	143.92263	50	Wujal Wujal	-15.969	145.315
21	Adavale	-25.909385	144.59863	51	Cungulla	-19.40177	147.11085
22	Capella	-23.086102	148.02308	52	Shoal Point	-21.0043	149.15302
23	Kalkadoon	-20.664824	139.49405	53	Tanbar	-26.32362	141.16899
24	Waverley	-21.225846	139.16252	54	Stokes	-18.68298	140.51475
25	Savannah	-19.148749	142.10074	55	Yarraden	-14.30771	143.30518
26	Suttor	-21.339211	147.9815	56	Holroyd River	-14.48995	142.82374
27	Saxby	-20.035225	142.48903	57	Archer River	-13.4291	142.94137
28	Three Rivers	-20.031009	140.03782	58	Lakefield	-14.93582	144.20547
29	Mckinlay	-21.272964	141.29449	59	South Wellesley Islands	-17.04611	139.41474
30	Moranbah	-22.002169	148.04624	60	Shelburne	-12.21983	142.58489
Dataset of 10 locations of Queensland used for Validation							
S.N	City	Lat(Deg.)	Long(Deg.)	S.N	City	Lat(Deg.)	Long(Deg.)
1	Tin Can Bay	-25.910843	153.00692	6	Gununa	-16.66676	139.17892
2	Lizard	-14.672757	145.45323	7	Evans Landing	-12.66237	141.84908
3	Portland Roads	-12.913764	143.02423	8	Stephens Island	-9.507367	143.54545
4	Injinoo	-11.057093	142.26278	9	Seisia	-10.85085	142.36611
5	Saibai Island	-9.38806	142.62587	10	Coconut Island	-10.05048	143.06906
Dataset of 15 locations of Queensland used for Testing							
S.N	City	Lat(Deg.)	Long(Deg.)	S.N	City	Lat(Deg.)	Long(Deg.)
1	Dixie	-15.11324	143.30567	9	Georgetown	-18.2918	143.54961
2	Maramie	-16.021241	142.40469	10	Paluma	-19.00886	146.20978
3	Highbury	-16.42556	143.14492	11	Sellheim	-20.00478	146.41978
4	Yagoonya	-16.426223	141.56236	12	Barkly	-20.46077	138.46859
5	Desailly	-16.484092	144.90196	13	Weerriba	-22.80178	150.63102
6	Paddys Green	-17.002578	145.37211	14	Glenfern	-26.96	152.61
7	Karron	-17.481504	141.89705	15	Adare	-27.512	152.296
8	Strathmore	-17.862329	142.55924				

Table 3. Predictor variables used for modeling after feature selection

S.N	Predictor Variable	Unit
1	Latitude	Deg
2	Air temperature	Deg C
3	Atmospheric pressure	kPa
4	Relative humidity	%
5	Daily solar radiation - horizontal	kWh/m²/d
6	Earth temperature	Deg C
7	Longitude	Deg

The MAE is the sum of absolute values of the errors divided by the number of observations. This quantity is often used in statistics as a measure how close calculated values are to measured values (Willmott & Matsuura, 2005) .

4. **Mean Bias error (MBE) is expressed as:**

$$MBE = \sum_{i=1}^{n} \frac{\left(ws_{FOR,i} - ws_{OBS,i}\right)}{N}$$

This indicator expresses the tendency of forecast model to underestimate (negative value) or overestimate (positive value) *Ws*. MBE values closest to zero are desirable. The drawback of this test is that it does not show the correct performance when the model presents overestimated and underestimated values at the same time, since overestimation and underestimation values cancel each other (Jiang, 2009).

5. **Willmott's Index (WI) is expressed as:**

$$WI = 1 - \left[\frac{\sum_{i=1}^{N} \left(ws_{FOR,i} - ws_{OBS,i}\right)^2}{\sum_{i=1}^{N} \left(\left| ws_{FOR,i} - \overline{ws}_{OBS,i} \right| + \left| ws_{OBS,i} - \overline{ws}_{OBS,i} \right| \right)^2} \right], 0 \le d \le 1$$

The index of agreement (Willmott Index; WI) which signifies the ratio between the mean square error and the "potential error" was computed to overcome the issue with *r*, RMSE and MAE.

6. **Relative root mean square error (RRMSE¸ %) is expressed as:**

$$RRMSE = \frac{\sqrt{\frac{1}{N}\sum_{i=1}^{N}\left(ws_{FOR,i} - ws_{OBS,i}\right)^2}}{\frac{1}{N}\sum_{i=1}^{N}\left(ws_{OBS,i}\right)} \times 100$$

RRMSE is calculated by dividing RMSE with the average value of the measured observational data. A model's precision level is excellent if the RRMSE < 10%, good if 10% < RRMSE < 20%, fair if 20% < RRMSE < 30% and poor if the RRMSE > 30% (Dawson, Abrahart, & See, 2007; Ravinesh C. Deo & Şahin, 2017; Jamieson, Porter, & Wilson, 1991; Moriasi, Arnold, Van Liew, Bingner, Harmel, & Veith, 2007; Shamshirband, Mohammadi, Chen, Narayana Samy, Petković, & Ma, 2015).

7. **Relative root Mean absolute error (RMAE), is expressed as:**

$$RMAE = \frac{1}{N}\sum_{i=1}^{N}\left|\frac{\left(ws_{FOR,i} - ws_{OBS,i}\right)}{ws_{OBS,i}}\right| \times 100$$

The RMAE when expressed as a percentage is also known as mean absolute percentage error (MAPE) (Yadav & Chandel, 2014). This indicator is expressed as the average absolute value of relative differences between estimated and measured windspeed.

8. **Nash–Sutcliffe coefficient (ENS), is expressed as:**

$$E_{NS} = 1 - \left[\frac{\sum_{i=1}^{N}\left(ws_{OBSi} - ws_{FORi}\right)^2}{\sum_{i=1}^{N}\left(ws_{OBSi} - \overline{ws}_{OBSi}\right)^2}\right], 0 \le E_{NS} \le 1$$

E_{NS} is a normalized statistic that governs the relative extent of the residual variance ("noise") compared to the measured data variance ("information") and provides a better assessment of a model as it is sensitive to differences in the observed and forecasted means and variances (Govindaraju, 2000).The closer the E_{NS} coefficient is to 1, the better the model's performance (Qiaofeng, Xu, Siyu, & Xiaohui, 2015).

9. **Legates and McCabe Index (E1), is expressed as:**

$$E_1 = 1 - \left[\frac{\sum_{i=1}^{N} ws_{OBSi} - ws_{FOR}{}^{i}}{ws_{OBSi} - \overline{ws}_{OBSi}}\right], 0 \le E_1 \le 1$$

Legates and McCabe (1999) suggested a modified index of agreement (E_1) that is less sensitive to high extreme values because errors and differences are given appropriate weighting by using the absolute value of the difference instead of using the squared differences (Legates & McCabe, 1999).

10. **Expanded uncertainty (U_{95}) expressed as:**

$$U_{95} = 1.96(SD^2 + RMSE^2)^{1/2}$$

Following Gueymard (Gueymard, 2014) and Behar et al.(Behar, Khellaf, & Mohammedi, 2015), this indicator is used in order to show more information about the model deviation. Where, 1.96 is the coverage factor corresponding to the 95% confidence level, and SD is the standard deviation of the difference between the calculated and measured data.

11. ***t*-statistic (*t*-stat) expressed as:**

$$t\text{-}stat = \sqrt{\frac{(N-1)MBE^2}{RMSE^2 - MBE^2}}$$

This indicator, which has had a long history of popular usage, was first proposed by Stone (Stone, 1993) to be used in combination with RMSE and MBE for more complete evaluation of models. For this research, *t*-statistics were used to validate whether the calculated values of windspeed are not significantly different from the measured observations. Better models have values closer to zero.

12. **Global Performance Indicator (GPI) expressed as:**

$$GPI = MBE \times RMSE \times U_{95} \times t_{stat} \times (1 - R^2)$$

The GPI is a multiplication of five statistical factors. These factors are less than unity. Therefore, the smaller the five statistics the smaller the GPI. The GPI combines the advantages of all the above-mentioned indicators because it examines the short and long term performance and linearity of the models. It can be used for ranking the models since it offers a higher resolution as its values are in the order of 10^{-5}. The first ranking model offers higher performance, with the highest modeling quality. The more the accuracy of the model, the closer to zero is the GPI (Stone, 1993).

3.4 ANN Implementation

This study uses the three-layer neural network for *Ws* simulation, where the first layer is the input layer representing predictor variables, the second layer is the hidden layer, and the third layer is the output layer. The number of input layers was seven variables (given by NCA feature selection). The selection of hidden neurons is the complicated part in ANN modelling, as it relates to the complexity of the system being modelled (Amirkhani, Nasirivatan, Kasaeian, & Hajinezhad, 2015; Quej, Almorox, Arnaldo, & Saito, 2017). By using the Equation [1] the initial number of neurons was calculated as 15 and a range

of 15–50 neurons were successively trialled until the output converged to a minimum Mean Square Error (MSE). In order to construct the best ANN model, the set of six back propagation training algorithms used were as follows: *trainlm, trainscg, traincgp, traincgf, trainoss* and *trainbfg*. Additionally, combinations of the input, hidden layer and output neurons of Equation [3] were tried one by one which resulted in a total of 54 ANN models being tested with different combinations of the transfer function (linear, hyperbolic-tangent sigmoid & log-sigmoid) for the hidden and output layer. As an additional measure, the correlation coefficient (*r*), RMSE and MAE of each trained model was noted to verify the model as detailed in Table 4. The ANN model with the Levenberg–Marquardt (LM) training function with *tansig* as sigmoid function for the input layer and *logsig* as sigmoid function for the output layer performed the best.

Table 4. Design parameters of artificial neural network (ANN) models with most appropriate 7 predictors, measured by correlation coefficient (r), root mean square error (RMSE) and mean absolute error (MAE).

S.N.	Training Function	Sigmoid Function Input	Sigmoid Function Output	Network Structure	r	RMSE (m/s)	MAE(m/s)
1	trainbfg	tansig	tansig	7-30-1	0.9509	0.2015	0.1541
2	trainbfg	tansig	purelin	7-45-1	0.9569	0.1885	0.1480
3	trainbfg	tansig	logsig	7-22-1	0.9546	0.1938	0.1522
4	trainbfg	purelin	tansig	7-24-1	0.8550	0.3588	0.2822
5	trainbfg	purelin	purelin	7-42-1	0.8597	0.3743	0.2953
6	trainbfg	purelin	logsig	7-48-1	0.8758	0.3281	0.2588
7	trainbfg	logsig	tansig	7-49-1	0.9495	0.2034	0.1613
8	trainbfg	logsig	purelin	7-35-1	0.9518	0.2013	0.1568
9	trainbfg	logsig	logsig	7-40-1	0.9510	0.2014	0.1549
10	traincgf	tansig	tansig	7-30-1	0.9574	0.1893	0.1458
11	traincgf	tansig	purelin	7-30-1	0.9455	0.2169	0.1644
12	traincgf	tansig	logsig	7-33-1	0.9395	0.2224	0.1732
13	traincgf	purelin	tansig	7-36-1	0.8437	0.3687	0.2937
14	traincgf	purelin	purelin	7-42-1	0.8584	0.3730	0.2946
15	traincgf	purelin	logsig	7-39-1	0.8564	0.3507	0.2710
16	traincgf	logsig	tansig	7-26-1	0.9423	0.2213	0.1691
17	traincgf	logsig	purelin	7-28-1	0.9376	0.2332	0.1807
18	traincgf	logsig	logsig	7-48-1	0.9494	0.2072	0.1591
19	traincgp	tansig	tansig	7-24-1	0.9424	0.2196	0.1686
20	traincgb	tansig	purelin	7-44-1	0.9408	0.2203	0.1715
21	trancgb	tansig	logsig	7-48-1	0.9570	0.1893	0.1459
22	trainscg	purelin	tansig	7-40-1	0.8564	0.3581	0.2853
23	trainscg	purelin	purelin	7-23-1	0.8556	0.3608	0.2850
24	trainrp	purelin	logsig	7-43-1	0.8670	0.3408	0.2646
25	trainrp	logsig	tansig	7-26-1	0.9423	0.2213	0.1691

continued on following page

Table 4. Continued

S.N.	Training Function	Sigmoid Function Input	Sigmoid Function Output	Network Structure	r	RMSE (m/s)	MAE(m/s)
26	trainoss	logsig	purelin	7-28-1	0.9375	0.2336	0.1821
27	trainoss	logsig	logsig	7-48-1	0.9494	0.2044	0.1563
28	trainlm	tansig	tansig	7-21-1	0.9591	0.1873	0.1468
29	trainlm	tansig	purelin	7-46-1	0.8733	0.3300	0.2593
30	**trainlm**	**tansig**	**logsig**	**7-46-1**	**0.9586**	**0.1874**	**0.1493**
31	trainlm	purelin	tansig	7-26-1	0.9581	0.2033	0.1605
32	trainlm	purelin	purelin	7-45-1	0.8656	0.5305	0.4402
33	trainlm	purelin	logsig	7-33-1	0.9122	0.2369	0.1875
34	trainlm	logsig	tansig	7-30-1	0.9554	0.1935	0.1473
35	trainlm	logsig	purelin	7-24-1	0.8625	0.4181	0.3237
36	trainlm	logsig	logsig	7-36-1	0.9617	0.1797	0.1389
37	trainoss	tansig	tansig	7-48-1	0.9451	0.2166	0.1726
38	traingdx	tansig	purelin	7-28-1	0.9382	0.2293	0.1761
39	traingdx	tansig	logsig	7-48-1	0.9582	0.1859	0.1447
40	traincgp	purelin	tansig	7-25-1	0.8497	0.3607	0.2873
41	traincgp	purelin	purelin	7-40-1	0.8537	0.3602	0.2840
42	traincgb	purelin	logsig	7-41-1	0.8471	0.3666	0.2852
43	traincgb	logsig	tansig	7-39-1	0.9248	0.2469	0.1971
44	trainscg	logsig	purelin	7-28-1	0.9345	0.2398	0.1842
45	trainscg	logsig	logsig	7-50-1	0.9451	0.2121	0.1601
46	trainscg	tansig	tansig	7-34-1	0.9467	0.2101	0.1576
47	trainrp	tansig	purelin	7-41-1	0.9386	0.2238	0.1770
48	trainrp	tansig	logsig	7-22-1	0.9557	0.1917	0.1527
49	trainoss	purelin	tansig	7-36-1	0.8506	0.3598	0.2863
50	trainoss	purelin	purelin	7-42-1	0.8544	0.3657	0.2887
51	traingdx	purelin	logsig	7-38-1	0.8571	0.3608	0.2822
52	traingdx	logsig	tansig	7-28-1	0.9357	0.2357	0.1776
53	traincgp	logsig	purelin	7-28-1	0.9369	0.2384	0.1847
54	traincgp	logsig	logsig	7-22-1	0.9547	0.1948	0.1551

3.5 GP Implementation

A total of 17 runs were performed with varying population sizes (50-50000) and parameter settings as shown in Table 5. The best GP model was selected for each location based on minimum RMSE on validation data. The performance of each best GP model was evaluated on training, validation and testing data. Table 6 shows the performance of the devloped GP model. The GP model yielded the best

results with a population size of 10,000. Equation [38] shows the MGGP model for the best GP model (Abbreviation used as per Table 1).

$$Model = 0.145\ P_{atm} - 3.46e^{-5}lat - 4.8e^{-6}I_{rad} + 2.57e^{-5}lat - 3.25e^{-5} *$$
$$\exp\left(\frac{-\left(1.0T_{air}\right)}{long}\right) - 0.263\exp\left(-1.0RH\right) - 0.33\tanh\left(E_{temp}\right)$$
$$+0.0136\exp(-1.0\exp(-1.0 * I_{rad}\ )1\ /\ 2) + 0.64lat + 4.12e^{-7}\tanh\left(\exp\left(-1.0P_{atm}\right)\right) *$$
$$(\tanh(lat) - 1.57)(-1.0long + E_{temp} + T_{air} - 3.72) + 0.324$$

4. RESULTS AND DISCUSSION

The measured and predicted values of Ws are plotted in Figure 5, it is clear that the predicted values are strongly correlated with the measured Ws data for the ANN model, with r ≈ 0.9545. ANN outperforms the GP model, with the correlation coeffecient of the GP model being r ≈ 0.8314. Similarly, the analysis of RMSE and MAE of the ANN models provide positive evidence that the ANN is better than GP. Table 4 and 6 demonstrate the comparisons of evaluation parameters for the predictive performance of ANN and GP. In this case, RMSE (≈ 0.177 -0.5305 ms^{-1}) and MAE (≈ 0.139- 0.44 ms^{-1}) were low for the ANN when compared to GP with RMSE (≈ 0.402-0.423 ms^{-1}) and MAE (≈ 0.302 -0.356 ms^{-1}).

The error histogram shows the variation of the error with instances. Figure 6 provides the authentication to the ANN model with the major part of the data coinciding with the zero error line when compared with GP. To have a better understanding of the model accuracy for practical applications, the frequency of the error encountered was determined in various error brackets. A histogram of the frequency of

Table 5. Parameter settings for the genetic programming (GP) model

Run Parameters	Value
Population size	50-50000
Number of generations	150
Number of runs	10
Parallel mode	off
Tournament size	80
Elite fraction	0.7
Fitness cache	enabled
Lexicographic selection	TRUE
Max tree depth	4
Max nodes per tree	Inf
Number of inputs	10
Max genes	10

Table 6. Design parameters of genetic programming (GP) models with most appropriate 7 predictors, measured by correlation coefficient (r), root mean square error (RMSE) and mean absolute error (MAE).

Population	r	RMSE (m/s)	MAE(m/s)
50	0.8030	0.4123	0.3429
200	0.7954	0.4194	0.3555
500	0.7953	0.4157	0.3237
800	0.8046	0.4024	0.3130
1000	0.8072	0.4065	0.3301
1500	0.8101	0.4243	0.3523
2000	0.8107	0.4037	0.3292
4000	0.8122	0.3946	0.3231
5000	0.8236	0.3950	0.3134
8000	0.8187	0.3919	0.3102
10000	**0.8314**	**0.3851**	**0.3016**
15000	0.7813	0.4208	0.3397
20000	0.7806	0.4202	0.3387
25000	0.8028	0.4039	0.3220
30000	0.8065	0.4080	0.3319
40000	0.7755	0.4207	0.3340
50000	0.8236	0.3950	0.3134

Figure 5. Regression plot of the ANN and GP (Note: The line in blue and red is the least-squares fit line to the respective scatter plots, r is correlation coefficient).

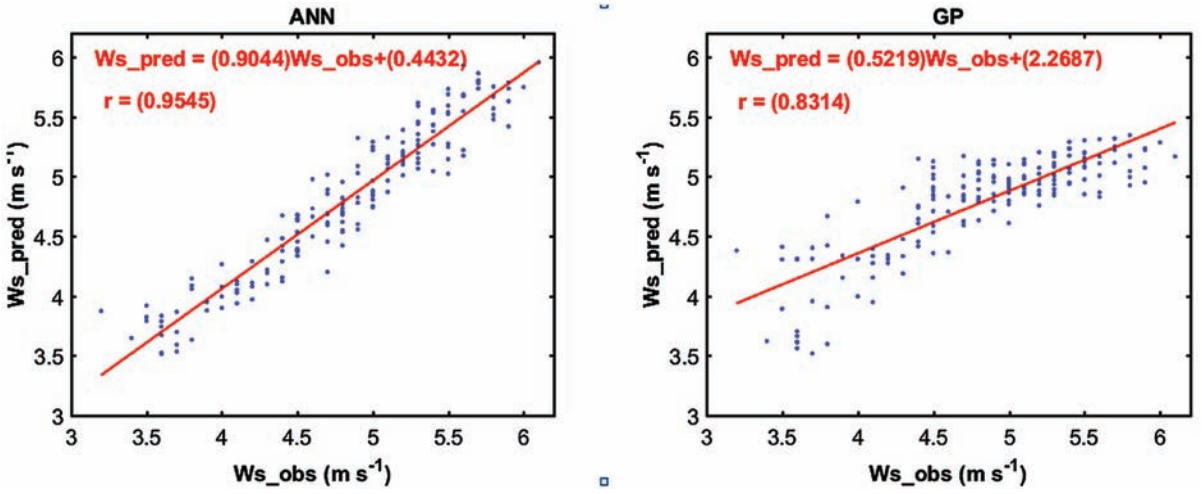

Figure 6. Error Histogram plot of artificial neural network and genetic programming model for all 15 testing locations. The vertical axis shows the frequencies of errors of each size on the horizontal axis.

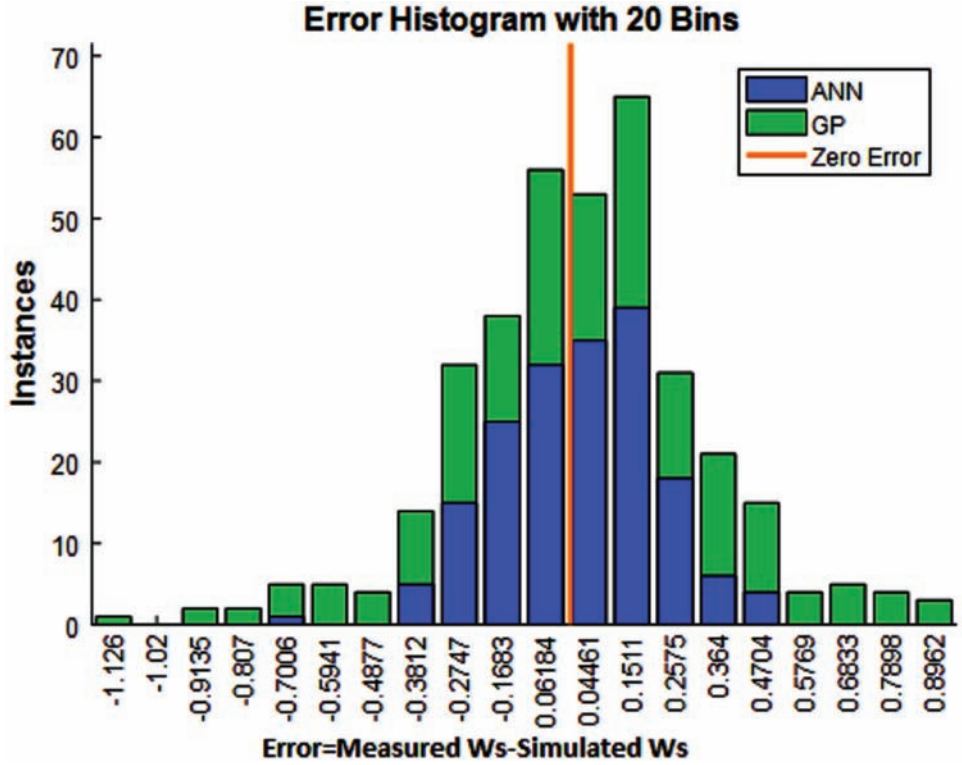

forecasted error (FE) with a ±0.1 $ms^{-1}day^{-1}$ error bracket has been prepared (Figure 7) Consistent with earlier results, the most correct forecasting is given by the ANN model. Remarkably, about 36% of the FE were seen to lie within the ± 0.1 ms^{-1}error range for ANN (Figure 5) whereas for the GP (Figure 8), the recorded FE was about 20% of all errors within ± 0.1 ms^{-1}. With ± 0.2 ms^{-1}ANN was also shown to be the better performing model with 71% of the FE falling within this error bracket.

The model assessment was also done using the normalized RMSE, RMAE and E_1 where the respective percentages are used. In agreement with previous findings, the ANN model outperformed the GP model. The graph of predictor metrics versus the model under study are shown in Fig. 9. The relative RMSE, RMAE, E_{NS} and E_1 are higher for the ANN model, indicating better performance. Other metrics in the same figure further indicate the better performance of ANN compared to GP, with the lowest GPI (≈ 0), *t*-stat (≈ 0.842), MBE (≈ 0.011) and U_{95} (≈ 0.519). Table 7 shows the measured and predicted values of *Ws* for the Queensland locations under study.

5. CONCLUSION

This study developed an ANN and GP model to predict the windspeed *(Ws)* of 15 locations in Queensland using metrological data from a total of 85 Queensland locations as forecast predictors. Moreover, the data was divided into training, validation and testing periods, including 60 locations for training, 10 for

Figure 7. Cumulative frequency of daily forecasting errors of Ws (m/s) for ANN model when all testing locations are pooled together, X-axis showing the forecasted error of Ws (ms^{-1}).

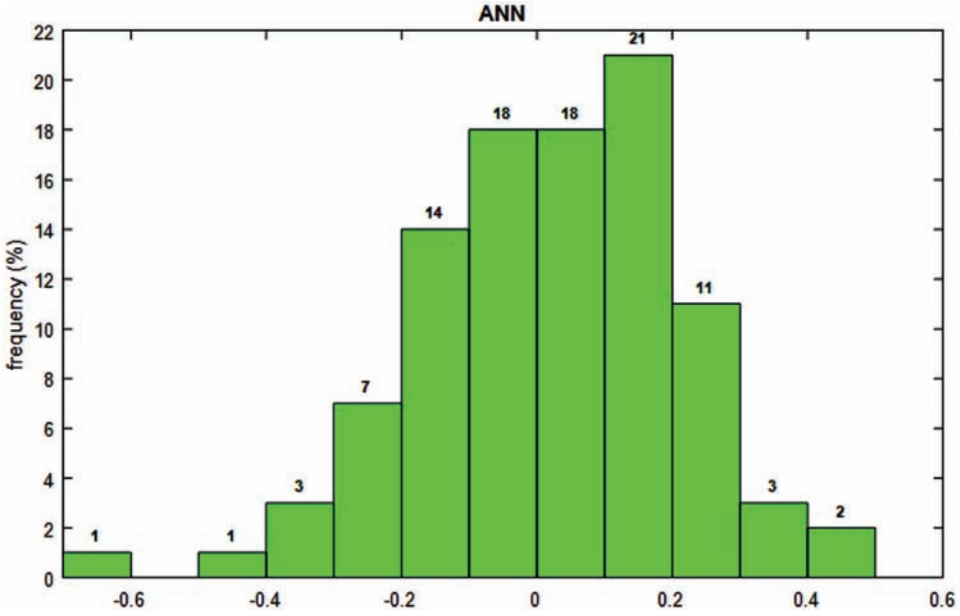

Figure 8. Cumulative frequency of daily forecasting errors of Ws (m/s) for GP model when all testing locations are pooled together, X-axis showing the forecasted error of Ws (ms^{1}).

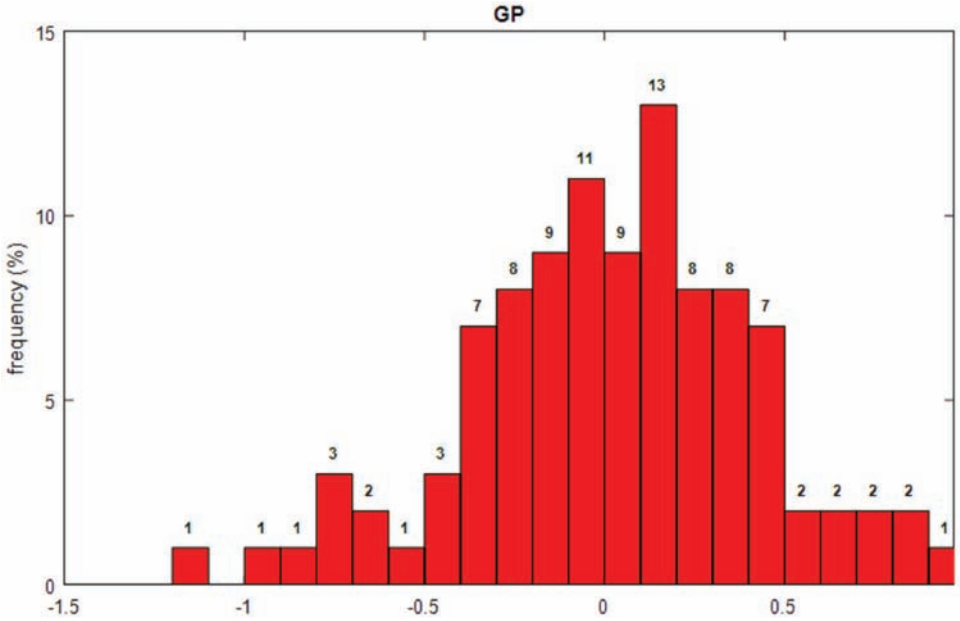

Figure 9. Predictor metrices comparison for the best ANN and GP model.

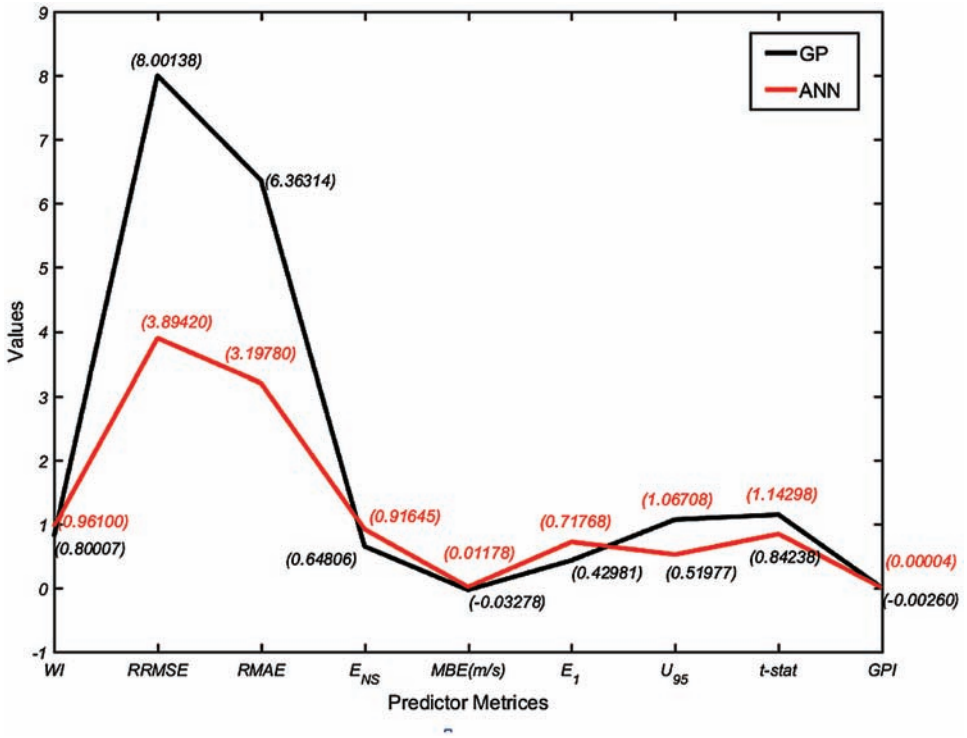

Table 7. Predicted Values of Windspeed using ANN and GP models

Location	Model	Jan	Feb	March	April	May	June	July	Aug	Sept	Oct	Nov	Dec
Dixie	Meas	4.40	4.70	5.30	5.80	5.70	5.50	5.70	5.70	6.10	5.70	5.20	4.80
	ANN	4.48	4.61	5.12	5.67	5.81	5.73	5.74	5.87	5.96	5.78	5.28	4.77
	GP	5.15	5.17	5.17	5.17	5.22	5.30	5.32	5.25	5.17	5.12	5.07	5.13
Maramie	Meas	4.50	4.70	5.30	5.60	5.40	5.10	5.30	5.30	5.80	5.40	5.10	4.80
	ANN	4.54	4.59	5.07	5.55	5.43	5.11	5.27	5.46	5.52	5.43	5.06	4.62
	GP	4.98	5.01	5.01	5.01	5.07	5.12	5.19	5.11	5.00	4.94	4.98	4.97
Highbury	Meas	4.50	4.80	5.40	5.80	5.50	5.20	5.40	5.40	5.90	5.50	5.20	4.90
	ANN	4.46	4.54	5.04	5.48	5.59	5.39	5.38	5.53	5.63	5.52	5.10	4.56
	GP	5.01	5.04	5.03	5.04	5.14	5.20	5.29	5.18	5.07	4.98	4.94	4.99
Yagoonya	Meas	4.70	5.00	5.40	5.80	5.90	5.50	5.60	5.30	5.60	5.30	5.20	5.00
	ANN	4.61	4.81	5.27	5.57	5.42	5.02	5.22	5.44	5.69	5.59	5.17	4.75
	GP	4.91	4.95	4.95	4.93	4.95	5.07	5.11	5.01	4.87	4.89	4.88	4.90
Desailly	Meas	4.50	4.90	5.50	5.90	5.60	5.30	5.50	5.50	6.00	5.60	5.30	5.00
	ANN	4.53	4.60	5.15	5.74	5.93	5.62	5.54	5.69	5.75	5.67	5.20	4.74
	GP	5.13	5.10	5.16	5.22	5.31	5.20	5.19	5.20	5.28	5.17	5.11	5.10

continued on following page

Table 7. Continued

Location	Model	Jan	Feb	March	April	May	June	July	Aug	Sept	Oct	Nov	Dec
Paddys Green	Meas	4.50	4.80	5.50	5.90	5.70	5.30	5.50	5.40	5.80	5.40	5.10	4.90
	ANN	4.63	4.71	5.27	5.79	5.79	5.26	5.25	5.56	5.75	5.55	5.15	4.78
	GP	5.08	5.10	5.12	5.24	5.32	5.08	5.09	5.24	5.35	5.23	5.14	5.14
Karron	Meas	4.50	4.60	5.10	5.30	5.20	4.80	5.00	4.90	5.30	5.00	4.90	4.70
	ANN	4.68	4.73	5.33	5.36	5.14	4.69	4.88	5.09	5.30	5.29	5.03	4.68
	GP	4.81	4.83	4.85	4.86	4.88	5.03	4.86	4.95	4.84	4.77	4.79	4.81
Strathmore	Meas	4.50	4.60	5.20	5.50	5.30	4.80	5.00	5.10	5.60	5.20	5.00	4.80
	ANN	4.38	4.50	5.01	5.25	5.11	4.77	4.84	5.10	5.18	5.12	4.86	4.55
	GP	4.85	4.83	4.85	4.85	4.94	4.89	4.91	5.00	4.83	4.76	4.80	4.78
Georgetown	Meas	4.50	4.50	5.10	5.20	5.00	4.40	4.80	4.80	5.30	5.10	4.90	4.70
	ANN	4.40	4.39	4.87	5.19	4.97	4.38	4.42	4.68	5.15	5.17	4.82	4.45
	GP	4.84	4.91	4.90	4.97	4.96	4.64	4.63	4.78	4.97	4.87	4.85	4.85
Paluma	Meas	4.50	4.30	5.10	5.20	4.90	3.80	4.70	4.70	5.10	5.00	5.00	4.50
	ANN	4.37	4.47	4.97	5.21	4.78	4.15	4.20	4.59	5.15	5.25	4.81	4.53
	GP	4.89	4.91	4.92	5.02	5.00	4.67	4.63	4.80	5.10	4.98	4.93	4.88
Sellheim	Meas	4.50	4.00	4.80	4.70	4.40	3.20	4.20	4.30	4.80	4.80	4.80	4.40
	ANN	4.34	4.26	4.70	4.69	4.29	3.87	3.97	4.22	4.82	4.95	4.74	4.42
	GP	4.71	4.79	4.78	4.92	4.74	4.38	4.34	4.48	4.97	4.81	4.79	4.75
Barkly	Meas	3.90	3.90	4.10	4.10	4.30	4.00	4.10	4.10	4.40	4.20	4.10	4.00
	ANN	3.96	3.95	4.13	4.10	4.10	3.90	4.05	3.94	4.16	4.29	4.03	3.99
	GP	4.33	4.34	4.33	4.40	4.33	4.00	3.95	4.15	4.45	4.32	4.28	4.31
Weerriba	Meas	4.50	4.70	5.00	4.90	4.70	4.50	4.60	4.50	4.80	4.60	4.70	4.40
	ANN	4.67	4.89	5.22	5.32	5.01	4.65	4.66	4.65	4.82	4.98	4.85	4.67
	GP	4.59	4.59	4.61	4.71	4.83	4.36	4.37	4.53	4.83	4.70	4.62	4.61
Glenfern	Meas	4.20	4.20	3.80	3.50	3.50	3.40	3.60	3.60	3.80	4.30	4.40	4.00
	ANN	4.08	4.11	4.06	3.92	3.79	3.65	3.67	3.79	4.09	4.19	4.12	4.07
	GP	4.27	4.31	4.42	4.41	3.89	3.62	3.61	3.62	3.91	4.19	4.42	4.31
Adare	Meas	3.50	3.60	3.70	3.70	3.60	3.60	3.80	3.70	3.60	3.70	3.90	3.60
	ANN	3.82	3.79	3.70	3.59	3.51	3.52	3.63	3.54	3.74	3.87	3.88	3.83
	GP	4.31	4.30	4.40	4.31	3.66	3.56	3.60	3.52	3.70	3.96	4.15	4.31

*Note:- Meas:- is measured windspeed in m/s /day

validation and 15 locations for testing. A total of eleven metrological data variables were extracted for the 85 locations from the publicly available NASA SSE6.0 dataset and optimised by the neighborhood component analysis (fsrnca) method of feature selection. In our study, we selected seven important predictor variables based on *'fsrnca"* which were: Latitude, Air temperature, Atmospheric Pressure, Relative Humidity, Daily Solar Radiation, Earth Temperature and Longitude.

A vast number of training algorithms and hidden transfer functions have been trailed in this study to achieve a prominent level of accuracy for the ANN model. The Levenberg–Marquardt backpropagation (*trainlm*) algorithm with tangent sigmoid functions for hidden neuron and logarithmic sigmoid as transfer function for the output was adopted for the best prediction of *Ws*. Further, the ANN model was compared with GP models. The iteration was done on the number of population sizes for the GP model. The enumeration of major findings and results showed:

1. The better performance of ANN model was evidenced in terms of high correlation coefficient $r \approx 0.9686$, low root mean square error, RMSE$\approx$0.188 ms^{-1} and low mean absolute error MAE$\approx$0.149 ms^{-1}, compared to low $r \approx 0.8314$, high RMSE$\approx$0.3851 ms^{-1} and high MAE$\approx$0.306 ms^{-1} for the optimal GP model.
2. In terms of normalized performance metrics, Willmott index WI and Nash-Sutcliffe coefficient E_{NS} attained by the optimal ANN was higher than the GP model. The values of these metrics were WI$\approx$0.961(ANN) and 0.647 (GP) and $E_{NS}\approx$0.916 (ANN), and 0.648 (GP) respectively. The Mean bias error for ANN was $\approx$ 0.0118 ms^{-1} compared to 0.0328 ms^{-1} for GP.
3. By assessing the performance of ANN in relation to GP using the most advanced normalized metrics of LegatesMcCabes (LM), the ANN again outperformed the optimal GP model. The obtained LM agreement values between the predicted *Ws* and observed *Ws* were LM$\approx$0.718 (ANN) and 0.430 (GP) respectively whereas the relative percentage errors RRMSE and RMAE ware only 3.89%, 3.19% (ANN) compared with 8.0%, 6.36% (GP).
4. In terms of expanded uncertainty $U_{95} \approx 0.52$, *t*-statistics (t-stat) $\approx$ 0.842 and global performance indicator GPI $\approx 4*10^{-5}$, the ANN model outperformed the GP model.

Concisely, this study advocates the possibility of using publicly available climate data with suitable feature selection methods to predict the windspeed *Ws*. Such a technique has useful application for renewable energy production and may be suited for selecting the best sites for development of wind power generators in the near future. The ANN model developed in this research can be optimized and tuned with other advanced techniques such as ensemble methods, particle swarm optimization PSO, genetic algorithms, fuzzy logic and so on. This study provides baseline information on the relevance of ANN at predicting local climatic factors., Other models such as support vector machine SVM and Extreme machine learning ELM which are built on and extend the commonly used ANN models may be utilized in future research to assess their potential for predicting windspeed in an Australian climate.

REFERENCES

Abhishek, K., Panda, B. N., Datta, S., & Mahapatra, S. S. (2014). Comparing Predictability of Genetic Programming and ANFIS on Drilling Performance Modeling for GFRP Composites. *Procedia Materials Science*, *6*, 544–550. doi:10.1016/j.mspro.2014.07.069

Abooali, D., & Khamehchi, E. (2014). Estimation of dynamic viscosity of natural gas based on genetic programming methodology. *Journal of Natural Gas Science and Engineering*, *21*, 1025–1031. doi:10.1016/j.jngse.2014.11.006

Afram, A., Janabi-Sharifi, F., Fung, A. S., & Raahemifar, K. (2017). Artificial neural network (ANN) based model predictive control (MPC) and optimization of HVAC systems: A state of the art review and case study of a residential HVAC system. *Energy and Building*, *141*, 96–113. doi:10.1016/j.enbuild.2017.02.012

Alexiadis, M. C., Dokopoulos, P. S., Sahsamanoglou, H. S., & Manousaridis, I. M. (1998). Short-term forecasting of wind speed and related electrical power. *Solar Energy*, *63*(1), 61–68. doi:10.1016/S0038-092X(98)00032-2

Amirkhani, S., Nasirivatan, S., Kasaeian, A. B., & Hajinezhad, A. (2015). ANN and ANFIS models to predict the performance of solar chimney power plants. *Renewable Energy*, *83*, 597–607. doi:10.1016/j.renene.2015.04.072

Behar, O., Khellaf, A., & Mohammedi, K. (2015). Comparison of solar radiation models and their validation under Algerian climate – The case of direct irradiance. *Energy Conversion and Management*, *98*, 236–251. doi:10.1016/j.enconman.2015.03.067

Benth, J. Š., & Benth, F. E. (2010). Analysis and modelling of wind speed in New York. *Journal of Applied Statistics*, *37*(6), 893–909. doi:10.1080/02664760902914490

Bilgili, M., & Sahin, B. (2013). Wind speed prediction of target station from reference stations data. *Energy Sources. Part A, Recovery, Utilization, and Environmental Effects*, *35*(5), 455–466. doi:10.1080/15567036.2010.512906

Blonbou, R. (2011). Very short-term wind power forecasting with neural networks and adaptive Bayesian learning. *Renewable Energy*, *36*(3), 1118–1124. doi:10.1016/j.renene.2010.08.026

Cadenas, E., & Rivera, W. (2007). Wind speed forecasting in the south coast of Oaxaca, Mexico. *Renewable Energy*, *32*(12), 2116–2128. doi:10.1016/j.renene.2006.10.005

Cadenas, E., & Rivera, W. (2010). Wind speed forecasting in three different regions of Mexico, using a hybrid ARIMA–ANN model. *Renewable Energy*, *35*(12), 2732–2738. doi:10.1016/j.renene.2010.04.022

Dawson, C. W., Abrahart, R. J., & See, L. M. (2007). HydroTest: A web-based toolbox of evaluation metrics for the standardised assessment of hydrological forecasts. *Environmental Modelling & Software*, *22*(7), 1034–1052. doi:10.1016/j.envsoft.2006.06.008

Dee, D. P., Uppala, S. M., Simmons, A. J., Berrisford, P., Poli, P., Kobayashi, S., ... Vitart, F. (2011). The ERA-Interim reanalysis: Configuration and performance of the data assimilation system. *Quarterly Journal of the Royal Meteorological Society*, *137*(656), 553–597. doi:10.1002/qj.828

Deo, R. C., & Sahin, M. (2017). Forecasting long-term global solar radiation with an ANN algorithm coupled with satellite-derived (MODIS) land surface temperature (LST) for regional locations in Queensland. *Renewable & Sustainable Energy Reviews*, *72*, 828–848. doi:10.1016/j.rser.2017.01.114

Despotovic, M., Nedic, V., Despotovic, D., & Cvetanovic, S. (2016). Evaluation of empirical models for predicting monthly mean horizontal diffuse solar radiation. *Renewable & Sustainable Energy Reviews*, *56*, 246–260. doi:10.1016/j.rser.2015.11.058

Elbayoumi, M., Ramli, N. A., & Fitri Md Yusof, N. F. (2015). Development and comparison of regression models and feedforward backpropagation neural network models to predict seasonal indoor PM2.5–10 and PM2.5 concentrations in naturally ventilated schools. *Atmospheric Pollution Research*, *6*(6), 1013–1023. doi:10.1016/j.apr.2015.09.001

Fan, G.-f., Wang, W.-s., & Liu, C. (2008). Wind power prediction based on artificial neural network. *Proceedings of the CSEE*, *34*, 118-123.

Farshad, F. F., Garber, J. D., & Lorde, J. N. (2000). Predicting temperature profiles in producing oil wells using artificial neural networks. *Engineering Computations*, *17*(6), 735–754. doi:10.1108/02644400010340651

Fletcher, R., & Reeves, C. M. (1964). Function minimization by conjugate gradients. *The Computer Journal*, *7*(2), 149–154. doi:10.1093/comjnl/7.2.149

Foley, A. M., Leahy, P. G., Marvuglia, A., & McKeogh, E. J. (2012). Current methods and advances in forecasting of wind power generation. *Renewable Energy*, *37*(1), 1–8. doi:10.1016/j.renene.2011.05.033

Garg, A., Vijayaraghavan, V., Mahapatra, S. S., Tai, K., & Wong, C. H. (2014). Performance evaluation of microbial fuel cell by artificial intelligence methods. *Expert Systems with Applications*, *41*(4), 1389–1399. doi:10.1016/j.eswa.2013.08.038

Gharbi, R., & Elsharkawy, A. (1996). Neural-network model for estimating the PVT properties of Middle East crude oils. *In Situ*, *20*(4), 367–394.

Gharbi, R., & Elsharkawy, A. M. (1997). *Neural network model for estimating the PVT properties of Middle East crude oils.* Paper presented at the Middle East Oil Show and Conference. 10.2118/37695-MS

Ghorbani, M., Khatibi, R., Hosseini, B., & Bilgili, M. (2013). Relative importance of parameters affecting wind speed prediction using artificial neural networks. *Theoretical and Applied Climatology*, *114*(1-2), 107–114. doi:10.100700704-012-0821-9

Govindaraju, R. S. (2000). Artificial neural networks in hydrology. II: Hydrologic applications. *Journal of Hydrologic Engineering*, *5*(2), 124–137. doi:10.1061/(ASCE)1084-0699(2000)5:2(124)

Gueymard, C. A. (2014). A review of validation methodologies and statistical performance indicators for modeled solar radiation data: Towards a better bankability of solar projects. *Renewable & Sustainable Energy Reviews*, *39*, 1024–1034. doi:10.1016/j.rser.2014.07.117

Hagan, M. T., Demuth, H. B., & Beale, M. H. (1996). Neural network design. PWS Pub. Co.

Hinchliffe, M., Hiden, H., McKay, B., Willis, M., Tham, M., & Barton, G. (1996). Modelling chemical process systems using a multi-gene. *Late Breaking Papers at the Genetic Programming*, 56-65.

Jamieson, P. D., Porter, J. R., & Wilson, D. R. (1991). A test of the computer simulation model ARCWHEAT1 on wheat crops grown in New Zealand. *Field Crops Research*, *27*(4), 337–350. doi:10.1016/0378-4290(91)90040-3

Jiang, Y. (2009). Estimation of monthly mean daily diffuse radiation in China. *Applied Energy*, *86*(9), 1458–1464. doi:10.1016/j.apenergy.2009.01.002

Kamble, L. V., Pangavhane, D. R., & Singh, T. P. (2015). Neural network optimization by comparing the performances of the training functions -Prediction of heat transfer from horizontal tube immersed in gas–solid fluidized bed. *International Journal of Heat and Mass Transfer*, *83*, 337–344. doi:10.1016/j.ijheatmasstransfer.2014.11.085

Kariniotakis, G., Stavrakakis, G., & Nogaret, E. (1996). Wind power forecasting using advanced neural networks models. *IEEE Transactions on Energy Conversion*, *11*(4), 762–767. doi:10.1109/60.556376

Kim, M. K. (2015). Short-term price forecasting of Nordic power market by combination Levenberg–Marquardt and Cuckoo search algorithms. *IET Generation, Transmission & Distribution*, *9*(13), 1553–1563. doi:10.1049/iet-gtd.2014.0957

Kobayashi, S., Ota, Y., Harada, Y., Ebita, A., Moriya, M., Onoda, H., ... Takahashi, K. (2015). The JRA-55 Reanalysis: General Specifications and Basic Characteristics. *Journal of the Meteorological Society of Japan. Ser. II*, *93*(1), 5–48. doi:10.2151/jmsj.2015-001

Koza, J. R. (1994). *Genetic Programming II Videotape: The Next Generation* (Vol. 55). MIT Press Cambridge.

Kriesel, D. (2007). *A brief Introduction on Neural Networks*. Academic Press.

Legates, D. R., & McCabe, G. J. Jr. (1999). Evaluating the use of "goodness-of-fit" measures in hydrologic and hydroclimatic model validation. *Water Resources Research*, *35*(1), 233–241. doi:10.1029/1998WR900018

Makinde, F., Ako, C., Orodu, O., & Asuquo, I. (2012). Prediction of crude oil viscosity using feed-forward back-propagation neural network (FFBPNN). *Petroleum and Coal*, *54*(2), 120–131.

Masrur, H., Nimol, M., Faisal, M., & Mostafa, S. M. G. (2016). *Short term wind speed forecasting using Artificial Neural Network: A case study.* Paper presented at the 2016 International Conference on Innovations in Science, Engineering and Technology (ICISET). 10.1109/ICISET.2016.7856485

MathWorks. (1996). *MATLAB: the language of technical computing: computation, visualization, programming: installation guide for UNIX version 5*. Natwick: Math Works Inc.

May, R., Dandy, G., & Maier, H. (2011). *Review of input variable selection methods for artificial neural networks*. INTECH Open Access Publisher. doi:10.5772/16004

Mohandes, M. A., Rehman, S., & Halawani, T. O. (1998). A neural networks approach for wind speed prediction. *Renewable Energy*, *13*(3), 345–354. doi:10.1016/S0960-1481(98)00001-9

Møller, M. F. (1993). A scaled conjugate gradient algorithm for fast supervised learning. *Neural Networks*, *6*(4), 525–533. doi:10.1016/S0893-6080(05)80056-5

Moriasi, D. N., Arnold, J. G., Van Liew, M. W., Bingner, R. L., Harmel, R. D., & Veith, T. L. (2007). Model evaluation guidelines for systematic quantification of accuracy in watershed simulations. *Transactions of the ASABE*, *50*(3), 885–900. doi:10.13031/2013.23153

Ojha, V. K., Dutta, P., Chaudhuri, A., & Saha, H. (2013). *Study of Various Conjugate Gradient Based ANN Training Methods for Designing Intelligent Manhole Gas Detection System.* Paper presented at the 2013 International Symposium on Computational and Business Intelligence. 10.1109/ISCBI.2013.24

Pham, D. T., & Sagiroglu, S. (2001). Training multilayered perceptrons for pattern recognition: A comparative study of four training algorithms. *International Journal of Machine Tools & Manufacture*, *41*(3), 419–430. doi:10.1016/S0890-6955(00)00073-0

Poli, R., Langdon, W., & McPhee, N. (2008). *A field guide to genetic programming*. Retrieved from http://lulu. *com*.

Qiaofeng, T., Xu, W., Siyu, C., & Xiaohui, L. (2015). *Daily runoff time-series prediction based on the adaptive neural fuzzy inference system.* Paper presented at the 2015 12th International Conference on Fuzzy Systems and Knowledge Discovery (FSKD).

Quej, V. H., Almorox, J., Arnaldo, J. A., & Saito, L. (2017). ANFIS, SVM and ANN soft-computing techniques to estimate daily global solar radiation in a warm sub-humid environment. *Journal of Atmospheric and Solar-Terrestrial Physics*, *155*, 62–70. doi:10.1016/j.jastp.2017.02.002

Rahdari, F., Eftekhari, M., & Mousavi, R. (2016). A two-level multi-gene genetic programming model for speech quality prediction in Voice over Internet Protocol systems. *Computers & Electrical Engineering*, *49*, 9–24. doi:10.1016/j.compeleceng.2015.10.008

Raja, M. A. (2008). *Real-time non-intrusive speech quality estimation of voice over internet protocol using genetic programming* (PhD thesis). Electronic and Computer Engineering, University of Limerick, Ireland.

Rienecker, M. M., Suarez, M. J., Gelaro, R., Todling, R., Bacmeister, J., Liu, E., ... Kim, G.-K. (2011). MERRA: NASA's modern-era retrospective analysis for research and applications. *Journal of Climate*, *24*(14), 3624–3648. doi:10.1175/JCLI-D-11-00015.1

Searson, D. P., Leahy, D. E., & Willis, M. J. (2010). GPTIPS: an open source genetic programming toolbox for multigene symbolic regression. *Proceedings of the International multiconference of engineers and computer scientists*.

Seo, K., & Hyeon, B. (2015). *Evolutionary nonlinear Model Output Statistics for wind speed prediction using Genetic Programming.* Paper presented at the 2015 7th International Joint Conference on Computational Intelligence (IJCCI).

Shamshirband, S., Mohammadi, K., Chen, H.-L., Narayana Samy, G., Petković, D., & Ma, C. (2015). Daily global solar radiation prediction from air temperatures using kernel extreme learning machine: A case study for Iran. *Journal of Atmospheric and Solar-Terrestrial Physics*, *134*, 109–117. doi:10.1016/j.jastp.2015.09.014

Sharma, B., & Venugopalan, K. (2014). Comparison of neural network training functions for hematoma classification in brain CT images. *IOSR-JCE*, *16*(1), 31–35. doi:10.9790/0661-16123135

Stackhouse, P., & Whitlock, C. (2009). *Surface meteorology and solar energy (SSE) release 6.0 Methodology, NASA SSE 6.0. In Earth Science Enterprise Program, National Aeronautic and Space Administration (NASA)*. Langley.

Staffell, I., & Green, R. (2014). How does wind farm performance decline with age? *Renewable Energy*, *66*, 775–786. doi:10.1016/j.renene.2013.10.041

Stone, R. J. (1993). Improved statistical procedure for the evaluation of solar radiation estimation models. *Solar Energy*, *51*(4), 289–291. doi:10.1016/0038-092X(93)90124-7

Ul-Saufie, A. Z., Yahaya, A. S., Ramli, N. A., Rosaida, N., & Hamid, H. A. (2013). Future daily PM 10 concentrations prediction by combining regression models and feedforward backpropagation models with principle component analysis (PCA). *Atmospheric Environment*, *77*, 621–630. doi:10.1016/j.atmosenv.2013.05.017

Willmott, C. J., & Matsuura, K. (2005). Advantages of the mean absolute error (MAE) over the root mean square error (RMSE) in assessing average model performance. *Climate Research*, *30*(1), 79–82. doi:10.3354/cr030079

Yadav, A. K., & Chandel, S. S. (2014). Solar radiation prediction using Artificial Neural Network techniques: A review. *Renewable & Sustainable Energy Reviews*, *33*, 772–781. doi:10.1016/j.rser.2013.08.055

Yang, W., Wang, K., & Zuo, W. (2012). Neighborhood Component Feature Selection for High-Dimensional Data. *JCP*, *7*(1), 161–168. doi:10.4304/jcp.7.1.161-168

Zameer, A., Arshad, J., Khan, A., & Raja, M. A. Z. (2017). Intelligent and robust prediction of short term wind power using genetic programming based ensemble of neural networks. *Energy Conversion and Management*, *134*, 361–372. doi:10.1016/j.enconman.2016.12.032

Zhu, X., & Genton, M. G. (2012). Short-Term Wind Speed Forecasting for Power System Operations. *International Statistical Review*, *80*(1), 2–23. doi:10.1111/j.1751-5823.2011.00168.x